

PROCONTEXT: EXPLORING PROGRESSIVE CONTEXT TRANSFORMER FOR TRACKING

Jin-Peng Lan^{1*}, Zhi-Qi Cheng^{2*}, Jun-Yan He^{1†}, Chenyang Li¹,
Bin Luo¹, Xu Bao¹, Wangmeng Xiang¹, Yifeng Geng¹, Xuansong Xie¹

¹DAMO Academy, Alibaba Group ²Carnegie Mellon University

ABSTRACT

Existing Visual Object Tracking (VOT) only takes the target area in the first frame as a template. This causes tracking to inevitably fail in *fast-changing* and *crowded scenes*, as it cannot account for changes in object appearance between frames. To this end, we revamped the tracking framework with **Progressive Context Encoding Transformer Tracker (ProContEXT)**, which coherently exploits *spatial and temporal contexts* to predict object motion trajectories. Specifically, ProContEXT leverages a context-aware self-attention module to encode the spatial and temporal context, refining and updating the multi-scale static and dynamic templates to progressively perform accurately tracking. It explores the complementary between spatial and temporal context, *raising a new pathway to multi-context modeling* for transformer-based trackers. In addition, ProContEXT revised the token pruning technique to reduce computational complexity. Extensive experiments on popular benchmark datasets such as GOT-10k and TrackingNet demonstrate that the proposed ProContEXT achieves state-of-the-art performance¹.

Index Terms— Context-aware transformer tracking

1. INTRODUCTION

Visual object tracking (VOT) is a crucial research topic due to its numerous applications, including autonomous driving, human-computer interaction, and video surveillance. In VOT, the goal is to predict the precise location of the target object in subsequent frames, given its location in the first frame, typically represented by a bounding box. However, due to challenges such as scaling and deformation, tracking systems must dynamically learn object appearance changes to encode content information. Additionally, in fast-changing and crowded scenes, visual trackers must identify which object to tracking among multiple similar instances, making tracking particularly challenging.

To address these challenges, we propose an intuitive solution. In Fig.1, we show three video frames chronologically in the first row, and their cropped patches are displayed below. The middle row of Fig.1 demonstrates that object appearance

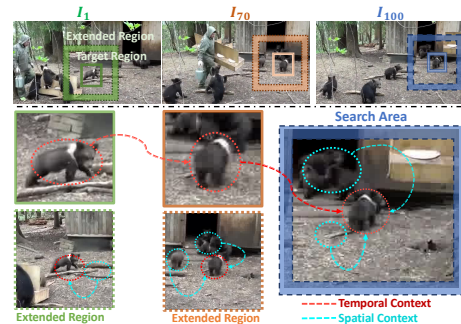


Fig. 1: The fast-changing and crowded scenes widely exist in visual object tracking. Apparently, exploiting the *temporal and spatial context* in video sequences is the cornerstone of accurate tracking.

can change significantly during tracking. The red dashed circles in the middle column represent the target object, which is more similar to objects in the search area, improving tracking performance. Furthermore, at the bottom of Fig. 1, we extend the template regions to include more background instances marked by cyan dotted circles, which could assist trackers in identifying similar targets. Thus, temporal and spatial contexts are crucial for visual object tracking, and we refer to them as *temporal context* and *spatial context*, respectively.

Despite the emergence of context-free tracking methods, such as Siamese-based trackers (e.g., SiamFC [1], SiamRPN [2], and SiamRPN++ [3]) and transformer-based approaches (e.g., TransT [4] and OTrack [5]), their performance suffers in rapidly changing scenarios due to the lack of contextual information. To address this, spatial context learning pipelines, such as TLD [6] and its extensions (e.g., LTCT [7], FuCoLoT [8], and LTT [9]), have been developed. Furthermore, dynamic template updating has been utilized in various tasks, including perception [10, 11], segmentation [12, 13], tracking [14–17], and density estimation [18, 19], for spatial context modeling. However, a comprehensive study of both temporal and spatial context in tracking tasks remains to be achieved.

To solve these issues, we propose a novel visual object tracking method called **Progressive Context Encoding Transformer Tracker (ProContEXT)**. ProContEXT encodes both temporal and spatial contexts through a template group composed of static and dynamic templates, providing a comprehensive and progressive context representation. The model leverages a context-aware self-attention module to learn rich and robust feature representations, while a tracking head

*equal contribution, alphabetically sorted

†corresponding author

¹The source code is at <https://github.com/jp-lan/ProContEXT>

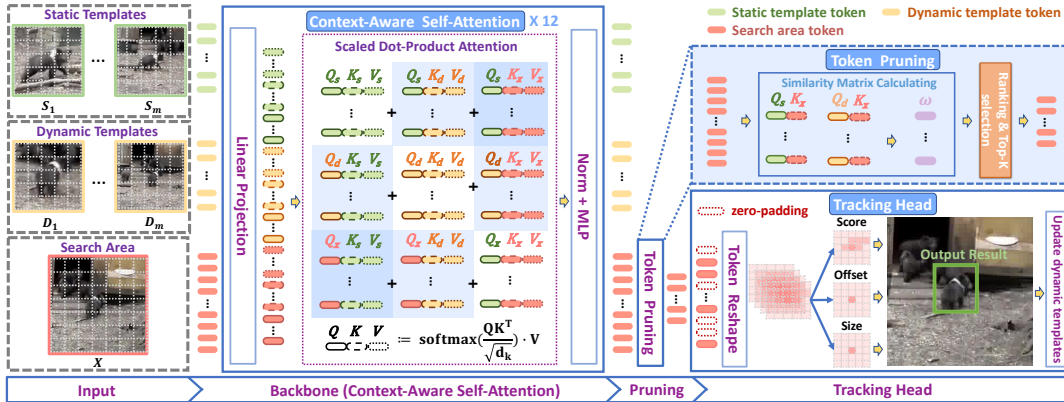


Fig. 2: The framework of Progressive Context Encoding Transformer Tracker (ProContEXT).

is used to update dynamic templates and generate tracking boxes. Furthermore, we adopt token pruning techniques to improve computational efficiency without compromising performance. The main contributions of this paper are:

- ProContEXT is the first work to exploit *progressive context encoding* over dynamic temporal and varying spatial in transformer-based tracking. It builds a *bridge between classical contextual tracking and context-free tracking*, and investigates how to encode context in real-time tracking.
- ProContEXT revises the ViT backbone, adding more *static and dynamic templates* and improving *context-aware self-attention* to exploit multi-temporal and multi-spatial information. With *progressive template refinement and updates*, it alters the *token pruning* to seamlessly bring contextual encoding into transformer-based tracking.
- ProContEXT *achieves SOTA performance* on large scale tracking benchmarks including TrackingNet [20] and GOT-10k [21]. Despite expanding long-term temporal and multi-scale spatial information, ProContEXT can *perform context encoding and tracking in real-time* at 54.3 FPS.

2. METHODOLOGY

2.1. Network Architecture

Unlike most previous works [2, 4, 5] that use only static templates at the first frame, ProContEXT aims to exploit templates of *multi-temporal and multi-spatial* to encode more context information.

Static & Dynamic Templates. As shown in Fig. 2, given video frames $\mathcal{V}=[I_1, \dots, I_n]$ and an initial box b_{init} , we crop the templates at different scales $\mathcal{K}=\{k_1, \dots, k_m\}$ to generate static templates $\mathcal{S}=\{S_1, \dots, S_m\}$, where S_t is cropped at scale k_t . Similarly, the dynamic templates $\mathcal{D}=\{D_1, \dots, D_m\}$ is produced to encode more object appearance changes during tracking. Following the standard setting [5, 16, 17, 22], we also crop the area centered on the box at the previous frame to get search area \mathcal{X} , assuming that the target object appears in the adjacent region of the last known location.² Overall,

²We’re abusing notation and symbolizing search areas and templates in the same way for ease of introduction.

we expand the dynamic templates with multi-temporal and multi-spatial details, which is plainly different from previous works that only use one static template.

Context-Aware Self-Attention. Based on the expanded dynamic templates, we modify the ViT [23] for representation learning. First, all templates $\mathcal{S} \cup \mathcal{D}$ and the search area \mathcal{X} are fed into a rescaling module for resizing. Then, each resized patch is cropped into non-overlapping 16×16 image patches, flattened to 1D, and positional embeddings are added after passing through the patch embedding layer. In the end, we encode \mathcal{S} , \mathcal{D} , and \mathcal{X} into static tokens $\mathcal{Z}_s=\{Z_s^1; \dots; Z_s^m\}$, dynamic tokens $\mathcal{Z}_d=\{Z_d^1; \dots; Z_d^m\}$, and search tokens $\mathcal{Z}_x=Z_x$, respectively. Then, all tokens are concatenated as $[\mathcal{Z}_s; \mathcal{Z}_d; \mathcal{Z}_x]$ and input coherently into the self-attention module as,

$$\begin{aligned}
 A(Q, K, V) &= \text{Softmax}\left(\frac{QK^T}{\sqrt{d_k}}\right) \cdot V \\
 &= \text{Softmax}\left(\frac{[Q_s; Q_d; Q_x][K_s; K_d; K_x]^T}{\sqrt{d_k}}\right) \cdot [V_s; V_d; V_x] \\
 &= \text{Softmax}\left(\frac{\begin{bmatrix} Q_s K_s^T & Q_s K_d^T & Q_s K_x^T \\ Q_d K_s^T & Q_d K_d^T & Q_d K_x^T \\ Q_x K_s^T & Q_x K_d^T & Q_x K_x^T \end{bmatrix}}{\sqrt{d_k}}\right) \cdot \begin{bmatrix} V_s \\ V_d \\ V_x \end{bmatrix}
 \end{aligned} \tag{1}$$

where Eq. (1) shows that the context-aware self-attention module can encode both dynamic temporal and variable spatial information from all static and dynamic templates. Diagonal terms, such as $Q_x K_x^T$, focus on the intra-region representation of the search area, while $Q_s K_s^T$ and $Q_d K_d^T$ fuse the spatial context in static templates and dynamic templates, respectively. Off-diagonal terms, such as $Q_s K_x^T$ and $Q_d K_x^T$, account for the interactions between templates and the search area. $Q_x K_s^T$ and $Q_x K_d^T$ aggregate the temporal context into the search areas, while $Q_s K_d^T$ and $Q_d K_s^T$ denote inter-template interactions. By leveraging 12 stacked attention layers, ProContEXT progressively extracts context-aware features.

Tracking Head. The tracking head consists of score head, offset head, and size head. After representation learning, only the tokens of the search area \mathcal{X} are reshaped into the 2D feature ($W_x \times H_x$), and fed into the tracking head. The reshaping here aims to convert 1D flattened tokens into the spatial

domain to perform the same tracking process as other convolutional networks. Specifically, the score head first gets a rough position and a score map. Then offset head and size head refine the offsets of position and box size on the resulting score map, respectively. More details are in Eq. (2-5 and corresponding descriptions).

Token Pruning. We modified the token pruning technique from previous works [5, 24] to accelerate ProContEXT. The purpose of pruning is to reduce computational costs by ignoring the search tokens for noisy background patches. Unlike OSTrack [5], which only considers the static template of the first frame, we take into account all static and dynamic templates. This allows foreground tokens to remain similar to dynamic templates even after significant changes in appearance. Moreover, the target object is usually located at the center point of the templates. If the similarity between the center point and the search token is low, the search token can be determined as the background. According to Eq. (1), the score of the search area token is computed by $\omega = \phi(\text{softmax}(Q_s K_x^T / \sqrt{d_k}) + \text{softmax}(Q_d K_x^T / \sqrt{d_k})) \in \mathbb{R}^{1 \times N_x}$, where N_x is the number of search tokens, and $\phi(\cdot)$ sums up the attention matrix that bonds to the template center tokens. Finally, we only keep the search tokens for the top-k elements of ω . The pruned tokens are replaced with zero-padding and then fed to the tracking head.

2.2. Training and Inference Settings

After presenting the architecture of ProContEXT, we now describe the training and inference settings.

Training Settings. Inspired by previous works [25], the training process is a progressive optimization process. First, the score head predicts the approximate location and score of the target object, where the Gaussian kernel generates the supervision as,

$$G_{xy} = \exp\left(-\frac{(x-p_x)^2 + (y-p_y)^2}{2\sigma_p^2}\right). \quad (2)$$

where (p_x, p_y) are the coordinates of the center point, and σ_p is the standard deviation that defines the size of the object. With the supervision of the Gaussian kernel, the score head is optimized with the focal loss [26],

$$L_s = -\sum \begin{cases} (1 - \hat{G}_{xy})^\alpha \log(\hat{G}_{xy}), & \text{if } G_{xy} = 1 \\ (1 - \hat{G}_{xy})^\beta (\hat{G}_{xy})^\alpha \log(1 - \hat{G}_{xy}), & \text{otherwise} \end{cases} \quad (3)$$

where $\hat{G}_{xy} \in [0, 1]^{W_x \times H_x}$ is the score map, (W_x, H_x) is the feature size of search area. We set $\alpha = 2$ and $\beta = 4$ as previous work [25]. After obtaining the maximum response of the score head $(\hat{x}, \hat{y}) = \text{argmax}_{x,y}(\hat{G}_{xy})$, the final predicted box can be computed as,

$$\hat{b} = (\hat{x} + \hat{\delta}_x, \hat{y} + \hat{\delta}_y, \hat{w}, \hat{h}) \quad (4)$$

where $(\hat{\delta}_x, \hat{\delta}_y)$ is the offset from the offset head, and (\hat{w}, \hat{h}) is the box size from the size head at location (\hat{x}, \hat{y}) , respectively. The bounding box obtained in Eq. 4 is trained with IoU loss [27] and L1 loss. Finally, the total loss can be noted as,

$$Loss = L_s + \lambda_{iou} L_{iou}(\hat{b}, b_{gt}) + \lambda_{l_1} L_1(\hat{b}, b_{gt}) \quad (5)$$

Algorithm 1 Inference with updating templates

```

1: Input: video frames  $\mathcal{V} = [I_1, \dots, I_n]$ , initial box  $b_{init}$ , scales  $\mathcal{K} = [k_1, \dots, k_m]$ , and trained ProContEXT();
2: Output: box for each frame  $\mathcal{B} = [b_1, \dots, b_n]$ ;
3: For each frame  $I_i$  in  $\mathcal{V}$  do
4:   if  $i == 1$  then
5:     Initialize templates  $\mathcal{S} = \text{crop}(I_1, b_{init}, \mathcal{K})$ ,  $\mathcal{D} = \mathcal{S}$ ;
6:     Initialize predicted box  $b_{pred} = b_{init}$ ;
7:   else
8:     Determine a search area  $\mathcal{X} = \text{crop}(I_i, b_{pred})$ ;
9:      $b_{pred}, score = \text{ProContEXT}(\mathcal{S}, \mathcal{D}, \mathcal{X})$ ; ▷ Eq. (4,6)
10:    if  $score > \tau$  then
11:       $\mathcal{D} = \{D_1, D_2, \dots, D_m\} = \text{crop}(I_i, b_{pred}, \mathcal{K})$ ;
12:    end if
13:  end if
14:  Update outputs  $\mathcal{B}[i] = b_{pred}$ ;
15: end for
16: return  $\mathcal{B} = [b_1, \dots, b_n]$ ;

```

where $\lambda_{iou} = 2$ and $\lambda_{l_1} = 5$ are the loss weights as in [17]. More details are in Sec. 3.2.

Inference Details. Unlike MixFormer [16] and STARK [17] that use an extra branch to update templates, we reuse the score head in inference. We take the maximum response of the score head as a confidence score,

$$score = \max(\hat{G}_{xy}) \quad (6)$$

where Alg. 1 depicts how to update the template in inference. After initializing static and dynamic templates (Line 5), confidence scale and position are used to assume whether to update the dynamic template (Line 8-9). Supposing that the confidence score is above a threshold τ (Line 10), the current tracking result b_{pred} is regarded as reliable and utilized to update the multi-scale dynamic templates progressively (Line 11).

3. EXPERIMENTS

3.1. Dataset and Metric

To conduct a thorough evaluation of the proposed ProContEXT, we utilize large-scale VOT benchmark datasets: TrackingNet [20] and GOT-10k [21]. The GOT-10k dataset includes more than 10,000 video segments and over 1.5 million manually labeled bounding boxes, while TrackingNet consists of 30,000 sequences with 14 million annotations. We adhere to the evaluation protocols of these datasets, with the average overlap (AO) and success rate (SR) used for evaluation on the train split of GOT-10k, and the area under the curve (AUC), precision, and normalized precision used for evaluation on TrackingNet. We also employ the same training datasets as recent state-of-the-art methods [5, 16, 17] when evaluating on TrackingNet.

3.2. Implementation Details

We implement the proposed ProContEXT using PyTorch and utilize the ViT-base backbone that is pre-trained by MAE [28]. Token pruning is conducted before the 4th, 7th, and 10th blocks at a keeping ratio of 0.7, which is consistent with [5, 24]. For training, we set the batch size and learning

Table 1: Comparison of State-of-the-Art (SOTA) Methods on TrackingNet [20] and GOT-10k [21] Datasets: The evaluated methods include "DT" (Dynamic Template) and "EB" (Extra Branch to update Dynamic Templates), along with different initialization methods, such as "Random-None" and pre-training with additional datasets, such as "CLIP-WIT [29]", "CLS-ImageNet-1k [30]", "CLS-ImageNet-22k [31]", or "MAE-ImageNet-1k [28]". The best performance is denoted in green font, and the corresponding performance increase is displayed in red font. When reporting results on the GOT-10k, trackers were only trained on the GOT-10k training split.

Method	Pre-training Method-Data	DT	EB	TrackingNet			GOT-10k		
				AUC	N-PRE	PRE	AO	SR _{0.5}	SR _{0.75}
SiamFC [1]	Random-None	×	-	57.1	66.3	53.3	34.8	35.3	9.8
SiamRPN++ [3]	Random-None	×	-	73.3	80.0	69.4	51.7	61.6	32.5
SimTrack [32]	CLIP-WIT	×	-	82.3	86.5	-	68.6	78.9	62.4
Simtrack [15]	CLS-ImageNet-1k	×	-	80.3	85.1	76.7	64.2	73.7	57.5
TransT [4]	CLS-ImageNet-1k	×	-	81.4	86.7	80.3	67.1	76.8	60.9
STARk [17]	CLS-ImageNet-1k	✓	✓	82.0	86.9	-	68.8	78.1	64.1
MixFormer [16]	CLS-ImageNet-1k	✓	✓	82.6	87.7	81.2	71.2	79.9	65.8
ProContEXT	CLS-ImageNet-1k	✓	×	83.4	88.3	82.2	72.0	82.7	68.0
MixFormer [16]	CLS-ImageNet-22k	✓	✓	83.1	88.1	81.6	70.7	80.0	67.8
ProContEXT	CLS-ImageNet-22k	✓	×	83.2	88.0	81.7	72.5	82.6	69.3
OTrack [5]	MAE-ImageNet-1k	×	-	83.9	88.5	83.2	73.7	83.2	70.8
ProContEXT	MAE-ImageNet-1k	✓	×	84.6	89.2	83.8	74.6	84.7	72.9
				↑+0.8	↑+0.6	↑+1.0	↑+0.8	↑+2.8	↑+2.2
				85.4	89.1	82.5	75.5	85.6	73.1
				↑+0.1	↓-0.1	↑+0.1	↑+1.8	↑+2.6	↑+1.5
				83.9	88.5	83.2	73.7	83.2	70.8
				84.6	89.2	83.8	74.6	84.7	72.9
				↑+0.7	↑+0.7	↑+0.6	↑+0.9	↑+1.5	↑+2.1

Table 2: Number of Scales for Static Templates: The best result is denoted in green font, and the corresponding increase is displayed in red font.

Method	scale num	\mathcal{K}	GOT-10k(val)	
			AO	SR _{0.5}
ProContEXT	1	[2.0]	85.1	94.6
	2	[2.0, 4.0]	86.7 ↑+1.6	96.5 ↑+1.9
	3	[2.0, 3.0, 4.0]	85.4 ↑+0.3	95.6 ↑+1.0
	4	[2.0, 2.7, 3.3, 4.0]	85.4 ↑+0.3	95.4 ↑+0.8

rate to 128 and 1e-4, respectively, and train the model using the AdamW solver for 300 epochs. We employ horizontal flip and template jittering in scale and size for data augmentations. All templates are resized to 192×192 , and the search area is resized to 384×384 for ProContEXT. During inference, the score threshold τ is set to 0.7. All experiments are conducted using 4 NVIDIA A100 GPUs.

3.3. Comparison with State-of-the-Art Methods

The performance comparison of the proposed ProContEXT with state-of-the-art methods on TrackingNet [20] and GOT-10k [21] is presented in Table 1. When pre-training with the ImageNet-1k dataset, ProContEXT achieves the best results among all compared methods. By utilizing MAE pre-training, ProContEXT outperforms the recent SOTA method, OTrack [5], by 0.9%, 1.5%, and 2.1% for AO, SR_{0.5}, and SR_{0.75} on GOT-10k [21], respectively. Furthermore, ProContEXT shows superior performance compared to methods [16, 17] that utilize an extra branch to update dynamic templates, while ProContEXT requires no additional branch and computation for updating dynamic templates. To validate the generalization ability of ProContEXT, we also evaluate our model on the TrackingNet [20] dataset, and it demonstrates better performance than the SOTA methods.

3.4. Ablation Study

We conduct an ablation study on the GOT-10k [21] benchmark. We rescale all the templates and the search area to 128×128 and 256×256 , respectively. We train ProContEXT for 100 epochs on the training split and report its performance on the validation split.

Investigation of Templates: To validate the effectiveness of spatial and temporal context, we analyzed the performance

Table 3: Exploration of Dynamic Templates: The best result is denoted in green font, and the corresponding increase is displayed in red font.

Method	\mathcal{K}	Dynamic template	GOT-10k(val)	
			AO	SR _{0.5}
ProContEXT	[2.0]		85.1	94.6
	[2.0]	✓	86.3 ↑+1.2	96.0 ↑+1.4
	[2.0, 4.0]	✓	86.8 ↑+1.7	96.8 ↑+2.2

Table 4: Exploration of Keeping Ratio ρ in Token Pruning: The best results and improvements are denoted in green and red font, respectively.

Method	ρ	GFLOPs	GOT-10k(val)	
			AO	SR _{0.5}
ProContEXT	0.6	36.1 ↓ 20.7%	85.8 ↑+0.1	95.4 ↑-0.1
	0.7	38.0 ↓ 16.5%	86.8 ↑+1.1	96.8 ↑+1.3
	0.8	40.1 ↓ 11.9%	86.3 ↑+0.3	96.1 ↑+0.6
	0.9	42.7 ↓ 6.2%	86.3 ↑+0.6	95.8 ↑+0.3
	1.0	45.5	85.7	95.5

of static and dynamic templates. For static templates, we investigated scale factors \mathcal{K} and scale numbers. The minimum scale factor of the template was set to 2, as in previous works [5, 17]. The maximum scale factor of the template was set to 4, which is the same as the search area. For different scale factor numbers, we uniformly distributed the scale factors between 2 and 4. From the results presented in Table 2, we observed that all models with multi-scale static templates enhanced performance since ProContEXT can effectively encode spatial context. Notably, ProContEXT with only one additional static template achieved the best result (+1.6% in AO and +1.9% in SR), suggesting that more static templates may introduce additional noise.

We also performed experiments to investigate the contribution of dynamic templates. From Table 3, it was evident that adding dynamic templates improved performance by 1.2% in AO and 1.4% in SR, demonstrating the effectiveness of temporal context. Furthermore, ProContEXT with both multi-scale static and dynamic templates achieved more than 2% improvement in SR, demonstrating the complementary nature of spatial and temporal context.

Effects of Token Pruning: Table 4 presents the effects of the token pruning module. The keeping ratio ρ indicates the proportion of reserved tokens after the pruning operation. As the value of ρ decreases, the computation amount decreases as well. When ρ is set to 0.7, ProContEXT improves AO by 1.1% and reduces GFLOPs by 16.5%, achieving a good trade-off between computation cost and accuracy.

4. CONCLUSION

In this work, we proposed the Progressive Context Encoding Transformer Tracker (ProContEXT) to revamp the visual object tracking framework. ProContEXT utilizes a context-aware self-attention module to encode spatial and temporal context, progressively refining and updating multi-scale static and dynamic templates for accurate tracking. Our extensive experiments on popular benchmark datasets such as GOT-10k and TrackingNet demonstrate that ProContEXT achieves state-of-the-art performance. In the future, we plan to explore more effective context-learning strategies and token-pruning schemes to reduce the impact of complex contexts.

5. REFERENCES

- [1] Luca Bertinetto, Jack Valmadre, João F. Henriques, Andrea Vedaldi, and Philip H. S. Torr, “Fully-convolutional siamese networks for object tracking,” in *ECCVW*, 2016, vol. 9914, pp. 850–865.
- [2] Bo Li, Junjie Yan, Wei Wu, Zheng Zhu, and Xiaolin Hu, “High performance visual tracking with siamese region proposal network,” in *CVPR*, 2018, pp. 8971–8980.
- [3] Bo Li, Wei Wu, Qiang Wang, Fangyi Zhang, Junliang Xing, and Junjie Yan, “Siamrpn++: Evolution of siamese visual tracking with very deep networks,” in *CVPR*, 2019, pp. 4282–4291.
- [4] Xin Chen, Bin Yan, Jiawen Zhu, Dong Wang, Xiaoyun Yang, and Huchuan Lu, “Transformer tracking,” in *CVPR*, 2021, pp. 8126–8135.
- [5] Botao Ye, Hong Chang, Bingpeng Ma, and Shiguang Shan, “Joint feature learning and relation modeling for tracking: A one-stream framework,” *arXiv:2203.11991*, 2022.
- [6] Zdenek Kalal, Krystian Mikolajczyk, and Jiri Matas, “Tracking-learning-detection,” *TPAMI*, vol. 34, no. 7, pp. 1409–1422, 2012.
- [7] Chao Ma, Xiaokang Yang, Chongyang Zhang, and Ming-Hsuan Yang, “Long-term correlation tracking,” in *CVPR*, 2015, pp. 5388–5396.
- [8] Alan Lukezic, Luka Cehovin Zajc, Tomás Vojtí, Jiri Matas, and Matej Kristan, “Fucolot - A fully-correlational long-term tracker,” in *ACCV*, 2018, vol. 11362, pp. 595–611.
- [9] Jack Valmadre, Luca Bertinetto, João F. Henriques, Ran Tao, Andrea Vedaldi, Arnold W. M. Smeulders, Philip H. S. Torr, and Efstratios Gavves, “Long-term tracking in the wild: A benchmark,” in *ECCV*, 2018, vol. 11207, pp. 692–707.
- [10] Chenyang Li, Zhi-Qi Cheng, Jun-Yan He, and et al., “Long-shortnet: Exploring temporal and semantic features fusion in streaming perception,” *arXiv:2210.15518*, 2022.
- [11] Zhi-Qi Cheng, Qi Dai, Siyao Li, Teruko Mitamura, and Alexander Hauptmann, “Gsrformer: Grounded situation recognition transformer with alternate semantic attention refinement,” in *ACM MM*, 2022, pp. 3272–3281.
- [12] Jian-Jun Qiao, Zhi-Qi Cheng, Xiao Wu, Wei Li, and Ji Zhang, “Real-time semantic segmentation with parallel multiple views feature augmentation,” in *ACM MM*, 2022, pp. 6300–6308.
- [13] Jun-Yan He, Shi-Hua Liang, Xiao Wu, Bo Zhao, and Lei Zhang, “Mgseg: Multiple granularity-based real-time semantic segmentation network,” *TIP*, vol. 30, pp. 7200–7214, 2021.
- [14] Yi Liu, Yanjie Liang, Qiangqiang Wu, Liming Zhang, and Hanzi Wang, “A new framework for multiple deep correlation filters based object tracking,” in *ICASSP*, 2022, pp. 1670–1674.
- [15] Zhihong Fu, Qingjie Liu, Zehua Fu, and Yunhong Wang, “Stm-track: Template-free visual tracking with space-time memory networks,” in *CVPR*, 2021, pp. 13774–13783.
- [16] Yutao Cui, Cheng Jiang, Limin Wang, and Gangshan Wu, “Mixformer: End-to-end tracking with iterative mixed attention,” in *CVPR*, 2022, pp. 13608–13618.
- [17] Bin Yan, Houwen Peng, Jianlong Fu, Dong Wang, and Huchuan Lu, “Learning spatio-temporal transformer for visual tracking,” in *ICCV*, 2021, pp. 10448–10457.
- [18] Zhi-Qi Cheng, Jun-Xiu Li, Qi Dai, Xiao Wu, and Alexander G Hauptmann, “Learning spatial awareness to improve crowd counting,” in *TCCV*, 2019, pp. 6152–6161.
- [19] Zhi-Qi Cheng, Qi Dai, Hong Li, Jingkuan Song, Xiao Wu, and Alexander G Hauptmann, “Rethinking spatial invariance of convolutional networks for object counting,” in *CVPR*, 2022, pp. 19638–19648.
- [20] Matthias Muller, Adel Bibi, Silvio Giancola, Salman Alsubaihi, and Bernard Ghanem, “Trackingnet: A large-scale dataset and benchmark for object tracking in the wild,” in *ECCV*, 2018, pp. 300–317.
- [21] Lianghua Huang, Xin Zhao, and Kaiqi Huang, “Got-10k: A large high-diversity benchmark for generic object tracking in the wild,” *TPAMI*, vol. 43, no. 5, pp. 1562–1577, 2021.
- [22] Zhi-Qi Cheng, Xiao Wu, Yang Liu, and Xian-Sheng Hua, “Video2shop: Exact matching clothes in videos to online shopping images,” in *CVPR*, 2017, pp. 4048–4056.
- [23] Alexey Dosovitskiy, Lucas Beyer, Alexander Kolesnikov, Dirk Weissenborn, Xiaohua Zhai, Thomas Unterthiner, Mostafa Dehghani, Matthias Minderer, Georg Heigold, Sylvain Gelly, et al., “An image is worth 16x16 words: Transformers for image recognition at scale,” *arXiv:2010.11929*, 2020.
- [24] Yongming Rao, Wenliang Zhao, Benlin Liu, Jiwen Lu, Jie Zhou, and Cho-Jui Hsieh, “Dynamicvit: Efficient vision transformers with dynamic token sparsification,” *NeurIPS*, vol. 34, pp. 13937–13949, 2021.
- [25] Xingyi Zhou, Dequan Wang, and Philipp Krähenbühl, “Objects as points,” *arXiv:1904.07850*, 2019.
- [26] Tsung-Yi Lin, Priya Goyal, Ross Girshick, Kaiming He, and Piotr Dollár, “Focal loss for dense object detection,” in *ICCV*, 2017, pp. 2980–2988.
- [27] Hamid Reza Tofighi, Nathan Tsoi, JunYoung Gwak, Amir Sadeghian, Ian Reid, and Silvio Savarese, “Generalized intersection over union: A metric and a loss for bounding box regression,” in *CVPR*, 2019, pp. 658–666.
- [28] Kaiming He, Xinlei Chen, Saining Xie, Yanghao Li, Piotr Dollár, and Ross Girshick, “Masked autoencoders are scalable vision learners,” *arXiv:2111.06377*, 2021.
- [29] Alec Radford, Jong Wook Kim, Chris Hallacy, Aditya Ramesh, Gabriel Goh, and et al., “Learning transferable visual models from natural language supervision,” in *ICML*, 2021, pp. 8748–8763.
- [30] Jia Deng, Wei Dong, Richard Socher, Li-Jia Li, Kai Li, and Li Fei-Fei, “Imagenet: A large-scale hierarchical image database,” in *CVPR*, 2009, pp. 248–255.
- [31] Tal Ridnik, Emanuel Ben-Baruch, Asaf Noy, and Lihit Zelnik-Manor, “Imagenet-21k pretraining for the masses,” *arXiv:2104.10972*, 2021.
- [32] Boyu Chen, Peixia Li, Lei Bai, Lei Qiao, Qihong Shen, Bo Li, Weihao Gan, Wei Wu, and Wanli Ouyang, “Backbone is all your need: A simplified architecture for visual object tracking,” *arXiv:2203.05328*, 2022.